A Numerical Investigation of TBA.....!!!1

By H.G.K.G Jayatunga

A thesis submitted to Monash University in fulfilment of the requirements for the Degree of

Doctor of Philosophy

Department of Mechanical Engineering
Monash University

Date ...!!!!!!

Contents

Chapter 1

A review of the literature

1.1 Flow induced vibrations

1.2 Fluid-elastic galloping

Fluid-elastic galloping is one of the most commonly observable flow-induced vibration on a slender body. Since this phenomenon is most common in civil structure, such as buildings and iced-transmission lines, the term “aeroelastic galloping” is commonly used as the body is immersed in air. However, this mechanism can occur on a slender body immersed in any Newtonian fluid, provided that the conditions to sustain the galloping mechanism are satisfied. This work is based on a general Newtonian flow,thus the term “ fluid-elastic galloping” is used throughout this thesis.

1.2.1 Excitation of galloping

Païdoussis et al. (2010) describes galloping as a “velocity dependent and damping controlled” phenomenon. Therefore, in order for a body to gallop, an initial excitation has to be given to that body. While this excitation is mainly caused by the force crated from vortex shedding, other fluid instabilities may contribute to this initial excitation. When a bluff body moves along the transverse direction of the fluid flow, it generates a force along the transverse direction. This force, also known as the induced lift is a resultant of the velocity of the fluid and the motion of the body. When this body is attached to an

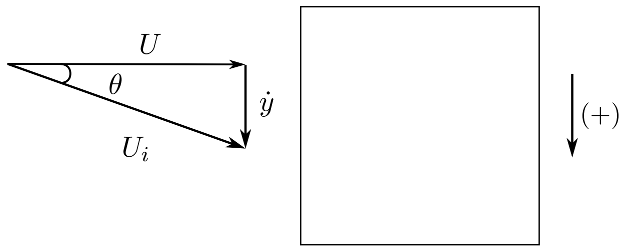

Figure 1.1: Induced angle of attack on the square prism due to the resultant of free-stream velocity of the fluid and transverse velocity of the body.

oscillating system (i.e. a simple spring, mass and damper system), the induced lift becomes the periodic forcing of the system. Galloping is sustained if the induced lift is in phase with the motion of the body. This could be explained further by using a square cross section as an example.

Figure 1.1 illustrates the motion of the body at a given instantaneous time.The induced angle of attack is formed on the square cross section as a result of the fressrteam velocity vector U and the transverse velocity vector of the body $\dot{y}$. Thus, a force is formed in phase with the motion of the body (square cross section). This mechanism could also be observed on other bodies which are prone to galloping. The sign convention in this figure (and generally used in this scope of research) states that downward direction is positive. Hence, the force generated on a body under the influence of galloping, could be also identified as a “negative lift”.

1.2.2 Quasi-steady state theory

According Païdoussis et al. (2010),the initial studies by Glauert (1919) provided a criterion for galloping by considering the auto-rotation of a stalled aerofoil. As this phenomenon commonly occur in iced transmission lines, Den Hartog (1956) has provided a theoretical explanation for iced electric transmission lines.

The pioneering study in order to mathematically model galloping was conducted by Parkinson and Smith (1964). This model has been widely used in almost all subsequent studies regarding galloping. A weakly non-linear oscillator model was developed by them to predict the response of the system. Essentially the quasi-steady assumption was made to develop this theory assuming that the instantaneous induced lift force of the oscillating body is equal to that of the lift force generated by the same body at the same induced angle of attack. In order to satisfy the quasi-steady assumption few conditions had to be satisfied.

- The velocity of the body does not change rapidly
- There is no interaction between vortex shedding and galloping

The second condition is satisfied by ensuring the vortex shedding frequency is much higher than the galloping frequency. The oscillator equation was solved using the Krylov and Bogoliubov method. Details of this method would not be mentioned as it is not used in the present study to solve the oscillator equation. The results obtained form experiments, carried out at $Re = 2200$ and a mass ratio (m^*) around 1164 had a good agreement with the theoretical data which is shown in figure 1.2.

Quasi-steady state oscillator model

The equation of motion of transversely oscillating body is given by

$$m\ddot{y} + c\dot{y} + ky = F_y, \tag{1.1}$$

where the forcing term F_y is given by

$$F_y = \frac{1}{2}\rho U^2 \mathcal{A} C_y. \tag{1.2}$$

As explained previously, when quasi-steady assumption is used the stationary C_y data (which consists of both lift and drag data) of the body could be could be used as inputs to the oscillator equation.Parkinson and Smith (1964) used a $7^t h$ order odd interpolating polynomial to determine C_y. The order of the polynomial can be chosen arbitrarily depending on the study. For example Barrero-Gil et al. (2009, 2010) have used a 3_{rd} order polynomial in order to simplify the analytical model. However, Ng et al. (2005) pointed out that a 7_{th} order polynomial is sufficient as it does not provide a significantly better result.

$$C_y(\theta) = a_1\left(\frac{\dot{y}}{U}\right) - a_3\left(\frac{\dot{y}}{U}\right)^3 + a_5\left(\frac{\dot{y}}{U}\right)^5 - a_7\left(\frac{\dot{y}}{U}\right)^7. \tag{1.3}$$

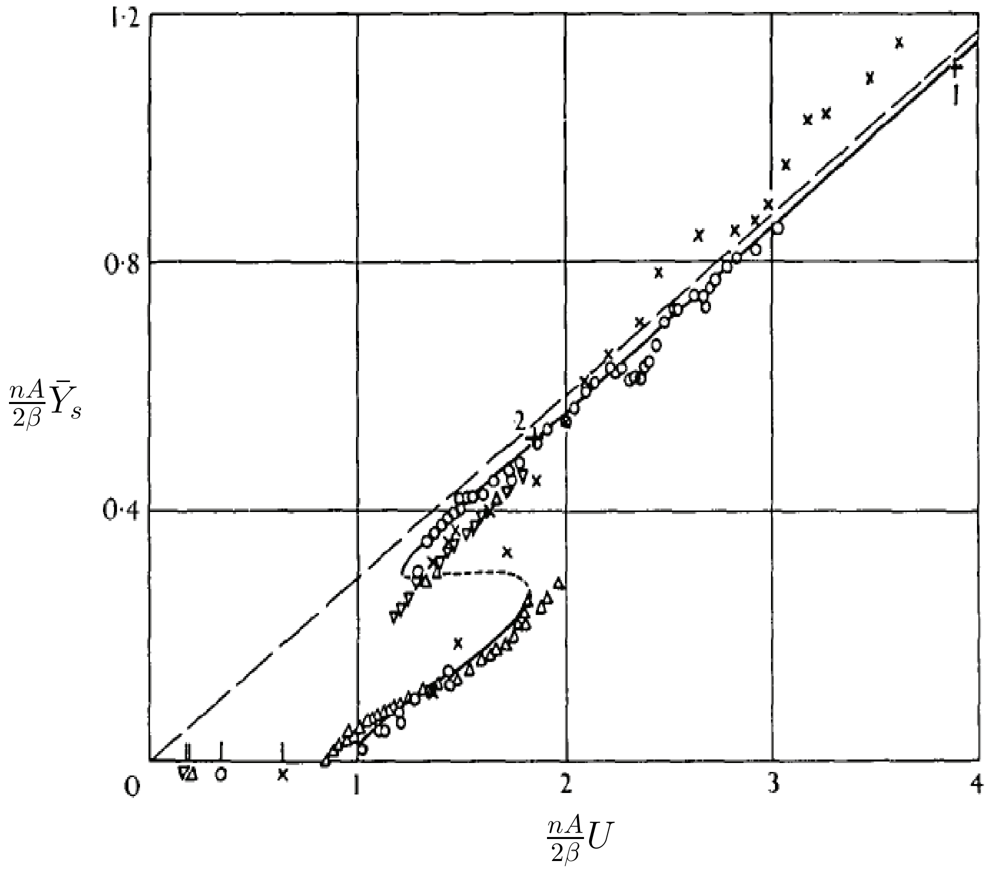

Figure 1.2: "Collapsed amplitude-velocity characteristic. Theory: ——— stable limit cycle, - - - unstable limit cycle. Experiment $\times$ β = .00107, $\circ$ β = .00196, $\triangle$ β = .00364,$\triangledown$ β = .00372, +1 β = .0012, +2 β = .0032 Reynolds numbers $4,000 - 20,000$ ". Figure extracted from Parkinson and Smith (1964). $\frac{nA}{2\beta}\bar{Y}_s$ is the dimensionless displacement amplitude parameter and $\frac{nA}{2\beta}U$ is the reduced velocity.

Therefore by substituting the forcing function to the oscillator equation (Eq:1.1) the Quasi-steady state (QSS) model could be obtained (Eq:1.4).

$$m\ddot{y}+c\dot{y}+ky=\frac{1}{2}\rho U^2\mathcal{A}\left(a_1\left(\frac{\dot{y}}{U}\right)-a_3\left(\frac{\dot{y}}{U}\right)^3+a_5\left(\frac{\dot{y}}{U}\right)^5-a_7\left(\frac{\dot{y}}{U}\right)^7\right). \tag{1.4}$$

As the current study is focused on the low Reregion, it is a known fact that the vortex shedding will be correlated well and therefore provide a significant forcing in the low Reynolds number region. Joly et al. (2012) introduced and additional sinusoidal forcing function to the model in order to integrate the forcing by vortex shedding. By the addition of this forcing Joly et al. (2012) managed to obtain accurate predictions of the displacement amplitude even at low mass ratios, where the galloping is suppressed or not present. Yet, the strength or the amplitude of this sinusoidal forcing has to be tuned in an *ad hoc* manner, and it was not clear the relationship between this forcing with the other system parameters. Thus in the current study this forcing was not used.

Presence of hysteresis

Hysteresis could be observed in the in the amplitude data of Parkinson and Smith (1964). In contrast, the studies carried out by Barrero-Gil et al. (2009) and Joly et al. (2012) at much lower Reynolds numbers ($159 \geq Re \leq 200$), did not show any hysteresis. Luo et al. (2003) concluded that the hysteresis was present due to the presence of an inflection point in the C_y curve at high Reynolds numbers (Parkinson and Smith (1964) data) which was not present at lower Reynolds numbers. It was further explained and demonstrated by Luo that the inflection point occurs due to the intermittent re attachment of the shear layer in certain angles at high Reynolds numbers.

1.2.3 Induced force and the shear layers

It is important to have an understanding on how the induced lift is generated in a fluid dynamics point of view. The quasi-steady model has already been validated and re-validated by many studies, therefore the flow-field data of static body simulations could be used to analyse the underpinning fluid dynamic mechanisms governing galloping.

The governing mechanism of galloping is the behaviour of the shear layers created at the leading edge due to flow separation on the top and bottom of the body. A common

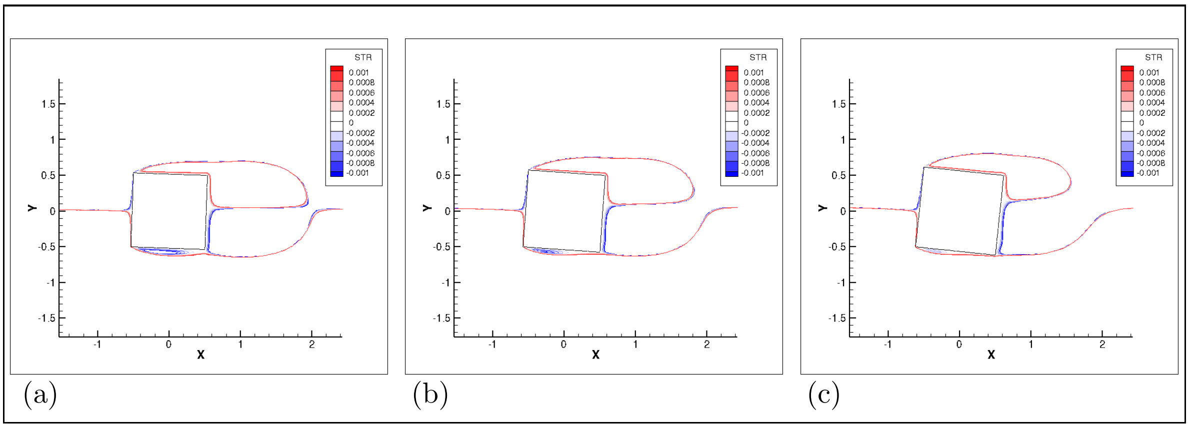

Figure 1.3: Stream functions of time averaged flow field on a stationary square section at $Re = 200$ at different incidence angles. (a) $2°$ (C_y increases),(b) $4°$ (C_y peaks) and (c) $2°$ (C_y decreases). The bottom shear layer comes closer to the bottom wall and reattaches as the angle of incidence increase.

example is a square cross section which has been used widely in studies on galloping. In this square cross section (figure 1.3) the flow separate from the leading edges of the body and create two shear layers on the top and bottom sides of the the body. Figure 1.3 shows the stream functions of time averaged (over a vortex shedding cycle) flow fields of stationary cross sections. The angle of incidence increases clockwise from $2° - 6°$. As θ is increased, the bottom shear comes closer to the wall of the body compared to the top shear layer (Figure 1.3 (a)). The shear layer nearer to the body crates higher suction compared to the shear layer at the opposite side. This pressure imbalance between the top and bottom sides of the body creates a downward force (i.e. the negative lift). As the angle is increased, the bottom shear layer becomes more closer and therefore the pressure difference becomes grater leading to a higher C_y. The negative lift force becomes maximum when the shear layer near to the wall reattaches at the trailing edge (figure 1.3 (b)). As θ is further increased, the bubble in the bottom shear layer shrinks in size resulting the reduction of the pressure imbalance of the top and bottom surface leading to the reduction in C_y. put the cY curve as crodd reference . As the body is connected to an oscillatory system (discussed in section 1.2.1), this shear layer behaviour also harmonize with the cyclic behaviour of the system providing the driving force to the system so that the motion of galloping is sustained.

1.2.4 Frequency response

It is clear that the cyclic motion of the shear layer harmonize with the mechanical system. Therefore, the frequency response should be then, the natural frequency of the system ω_n which much is different from VIV mechanism, where the primary frequency comes from the periodic forcing of the vortex shedding. Hence, in the QSS model the natural frequency of the system could be identified as the frequency of oscillations. However, it should be noted that this is valid on the regimes where the conditions discussed in section 1.2.2 are satisfied.

On the other hand, the forcing function in the QSS model equation 1.4, is a non linear function. As the mass ratio is quite high, the non-linearities of the forcing does not make much effect to the frequency response. However, as the mass ratio goes down theoretically the non linearities of the forcing should affect the frequency response of the system.

The experimental studies carried by Bouclin (1977) concluded at high reduced velocities with large inertia, the motion of the cylinder controls the frequency of the system rather than the vortex shedding. The structural damping has no effect provided that it is small. He also concluded that as the inertia and the reduced velocity gets lower, there is some interaction between vortex shedding and galloping. And at this region the frequency is mainly governed by the vortex shedding.

1.2.5 Fluid mechanics governing the galloping response

As discussed in subsection 1.2.3 the driving force of a galloping system is the asymmetrical placement of the shear layers at either sides of the body. In consequence, it is clear that a significant afterbody is needed for the shear layer interaction to sustain galloping. Manipulating the shape of the afterbody and thereby, manipulating the shear layer interactions with the body, gives the ability to control the galloping response. Thus, due to this reason work has been carried out on the response of galloping of different cross sectional shapes.

Section	h/d	$\partial C_{F_y}/\partial\alpha$ Smooth flow	$\partial C_{F_y}/\partial\alpha$ Turbulent flow[b]	Reynolds number
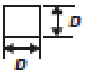	1	3.0	3.5	10^5
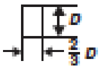	3/2	0.	−0.7	10^5
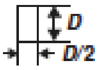	2	−0.5	0.2	10^5
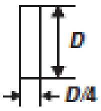	4	−0.15	0.	10^5
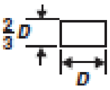	2/3	1.3	1.2	6.6×10^4
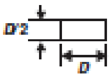	1/2	2.8	−2.0	3.3×10^4
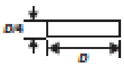	1/4	−10.	–	$2 \times 10^3 - 2 \times 10^4$
 (Thin airfoil)	–[c]	−6.3	−6.3	$>10^3$
	–	−6.3	−6.3	$>10^3$
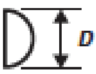	–	−0.1	0.	6.6×10^4
	–	−0.5	2.9	5.1×10^4
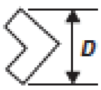	–	0.66	–	7.5×10^4

[a] α is in radians; flow is left to right. $\partial C_{F_y}/\partial\alpha = -\partial C_L/\partial\alpha - C_D$, with C_{F_y} based on the dimension D, so that $\partial C_{F_y}/\partial\alpha > 0$ for galloping.
[b] Approximately 10% turbulence.
[c] Inappropriate to use h/d.

Figure 1.4:

Bibliography

Barrero-Gil, A., Alonso, G., Sanz-Andres, A., Jul. 2010. Energy harvesting from transverse galloping. Journal of Sound and Vibration 329 (14), 2873–2883.

Barrero-Gil, A., Sanz-Andrés, A., Roura, M., Oct. 2009. Transverse galloping at low Reynolds numbers. Journal of Fluids and Structures 25 (7), 1236–1242.

Bouclin, D. N., 1977. Hydroelastic oscillations of square cylinders. Master's thesis, University of British Columbia.

Den Hartog, J. P., 1956. Mechanical Vibrations. Dover Books on Engineering. Dover Publications.

Glauert, H., 1919. The rotation of an aerofoil about a fixed axis. Tech. rep., Advisory Committee on Aeronautics R and M 595. HMSO, London.

Joly, A., Etienne, S., Pelletier, D., Jan. 2012. Galloping of square cylinders in cross-flow at low Reynolds numbers. Journal of Fluids and Structures 28, 232–243.

Luo, S., Chew, Y., Ng, Y., Aug. 2003. Hysteresis phenomenon in the galloping oscillation of a square cylinder. Journal of Fluids and Structures 18 (1), 103–118.

Ng, Y., Luo, S., Chew, Y., Jan. 2005. On using high-order polynomial curve fits in the quasi-steady theory for square-cylinder galloping. Journal of Fluids and Structures 20 (1), 141–146.

Païdoussis, M., Price, S., de Langre, E., 2010. Fluid-Structure Interactions : Cross-Flow-Induced Instabilities. Cambridge University Press.

Parkinson, G. V., Smith, J. D., 1964. The square prism as an aeroelastic non-linear oscillator. The Quarterly Journal of Mechanics and Applied Mathematics 17 (2), 225–239.